Report

Current Biology

Competing beetles attract egg laying in a hawkmoth

Highlights

- Female moths prefer to lay their eggs on beetle-infested plants
- α-Copaene plays a critical role in attracting moth oviposition
- Moths make such decisions to benefit from reduced attack rate from parasitoid wasps
- Odorant receptor 35 is involved in detecting α-copaene

Authors

Jin Zhang, Syed Ali Komail Raza, Zhiqiang Wei, ..., Jonathan Gershenzon, Markus Knaden, Bill S. Hansson

Correspondence

mknaden@ice.mpg.de (M.K.), hansson@ice.mpg.de (B.S.H.)

In brief

Zhang et al. show that *Manduca sexta* prefers to lay its eggs on beetle-infested plants. Caterpillars feeding on these plants have a reduced chance of being parasitized by wasps. The authors show that the beetle-induced plant volatile α-copaene can elicit moth oviposition and the odorant receptor 35 is involved in its detection.

Zhang et al., 2022, Current Biology *32*, 861–869
February 28, 2022
https://doi.org/10.1016/j.cub.2021.12.021

CellPress

Current Biology

CellPress
OPEN ACCESS

Report

Competing beetles attract egg laying in a hawkmoth

Jin Zhang,[1] Syed Ali Komail Raza,[1] Zhiqiang Wei,[2] Ian W. Keesey,[1] Anna L. Parker,[3] Felix Feistel,[4] Jingyuan Chen,[4] Sina Cassau,[5] Richard A. Fandino,[1,6] Ewald Grosse-Wilde,[1,7] Shuanglin Dong,[2] Joel Kingsolver,[3] Jonathan Gershenzon,[4] Markus Knaden,[1,8,9,*] and Bill S. Hansson[1,8,*]

[1]Department of Evolutionary Neuroethology, Max Planck Institute for Chemical Ecology, Hans-Knöll-Straße 8, 07745 Jena, Germany
[2]Key Laboratory of Integrated Management of Crop Disease and Pests, Ministry of Education/Department of Entomology, College of Plant Protection, Nanjing Agricultural University, Weigang No. 1, 210095 Nanjing, China
[3]Department of Biology, The University of North Carolina at Chapel Hill, Chapel Hill, NC 27599, USA
[4]Department of Biochemistry, Max Planck Institute for Chemical Ecology, Hans-Knöll-Straße 8, 07745 Jena, Germany
[5]Institute of Biology/Zoology, Department of Animal Physiology, Martin Luther University Halle-Wittenberg, 06120 Halle (Saale), Germany
[6]Department of Ecology and Evolutionary Biology, Cornell University, Dale R. Corson Hall, Ithaca, NY 14853, USA
[7]EXTEMIT-K, Faculty of Forestry and Wood Sciences, Czech University of Life Sciences Prague, Kamýcká 129, 165 00 Praha-Suchdol, Czech Republic
[8]Senior author
[9]Lead contact
*Correspondence: mknaden@ice.mpg.de (M.K.), hansson@ice.mpg.de (B.S.H.)
https://doi.org/10.1016/j.cub.2021.12.021

SUMMARY

In nature, plant-insect interactions occur in complex settings involving multiple trophic levels, often with multiple species at each level.[1] Herbivore attack of a host plant typically dramatically alters the plant's odor emission in terms of concentration and composition.[2,3] Therefore, a well-adapted herbivore should be able to predict whether a plant is still suitable as a host by judging these changes in the emitted bouquet. Although studies have demonstrated that oviposition preferences of successive insects were affected by previous infestations,[4,5] the underlying molecular and olfactory mechanisms remain unknown. Here, we report that tobacco hawkmoths (*Manduca sexta*) preferentially oviposit on Jimson weed (*Datura wrightii*) that is already infested by a specialist, the three-lined potato beetle (*Lema daturaphila*). Interestingly, the moths' offspring do not benefit directly, as larvae develop more slowly when feeding together with *Lema* beetles. However, one of *M. sexta*'s main enemies, the parasitoid wasp *Cotesia congregata*, prefers the headspace of *M. sexta*-infested plants to that of plants infested by both herbivores. Hence, we conclude that female *M. sexta* ignore the interspecific competition with beetles and oviposit deliberately on beetle-infested plants to provide their offspring with an enemy-reduced space, thus providing a trade-off that generates a net benefit to the survival and fitness of the subsequent generation. We identify that α-copaene, emitted by beetle-infested *Datura*, plays a role in this preference. By performing heterologous expression and single-sensillum recordings, we show that odorant receptor (Or35) is involved in α-copaene detection.

RESULTS AND DISCUSSION

Beetle-infested *Datura* attract female *M. sexta* for oviposition

L. daturaphila (Coleoptera: Chrysomelidae), which occurs sympatrically and concurrently with *M. sexta*, is the primary herbivore of the sacred Jimson weed, *D. wrightii*.[6,7] *L. daturaphila* and *M. sexta* are often found on the same or neighboring plants of *D. wrightii* in central and south California.[8] During field trips, we have identified *L. daturaphila* and *M. sexta* multiple times at various locations in Utah and Arizona. *Lema* larvae aggregate and cover themselves with their feces, probably as a result of defensive adaptations.[9] It has been shown that the infestation of *Datura* by *Lema* induces the emission of great amounts of HIPVs.[10] As beetles and *M. sexta* larvae may compete for food resources, we hypothesized that female *M. sexta* would avoid ovipositing on beetle-infested plants.

We first tested the behavioral response of gravid *M. sexta* females toward beetle-larvae-infested plants in a two-choice assay in a wind tunnel (Figure 1A). Contrary to our initial hypothesis, 17/21 of *M. sexta* females contacted the beetle-larvae-infested plants first and laid significantly more eggs on them compared with control plants (Figure 1C). Notably, *M. sexta* females showed a similar preference to plants infested by adult beetles (Figure 1D). To test whether this preference was due to the actual presence of beetle larvae/adults or to the effect of the beetle herbivory, we tested again after removing beetles from the infested plants. Indeed, female *M. sexta* preferred the previously infested plants to the control (Figure 1E). However, when we placed beetles on undamaged plants right before the wind tunnel test, female moths ignored the

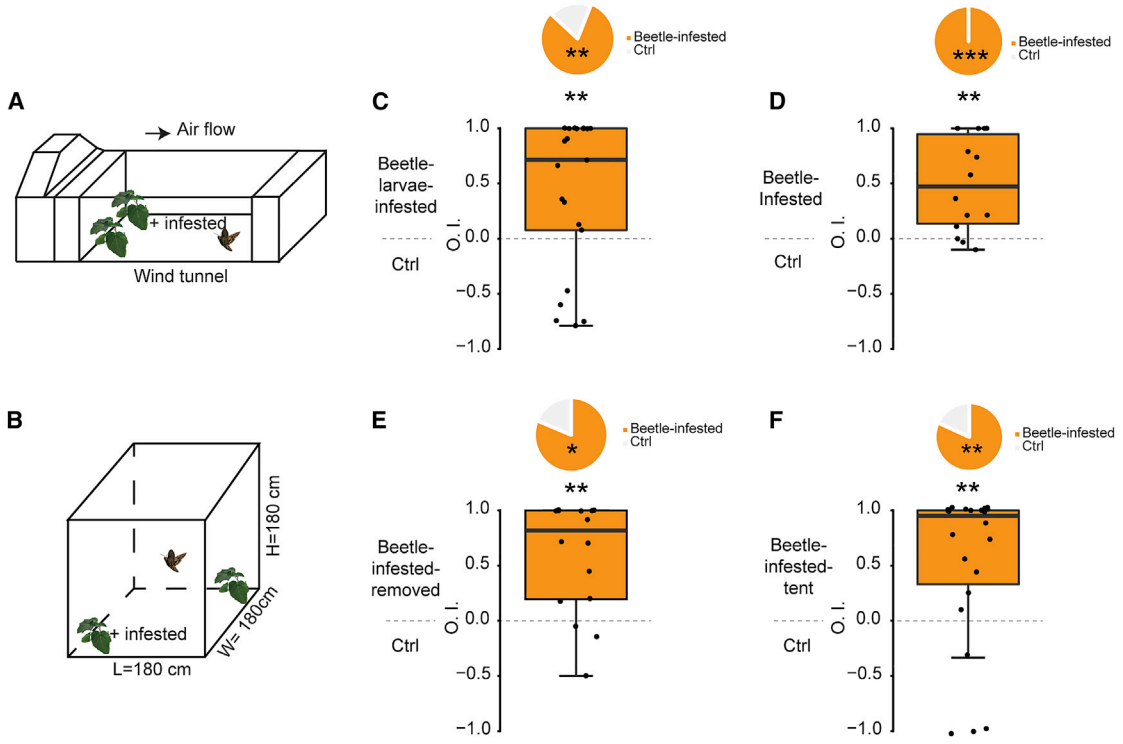

Figure 1. *M. sexta* finds the beetle-infested plants more attractive

(A and B) Schematic drawing of wind tunnel assay (WTA) (A) and tent assay (TA) (B).

(C) Oviposition indices—O. I. = (number of eggs on treatment − number of eggs on control)/total egg number—from WTA between beetle-larvae-infested and control.

(D) O. I. from WTA between beetle-infested and control.

(E) O. I. from WTA between beetle-infested with beetles removed and control.

(F) O. I. from TA between beetle-infested and control.

Pie charts depict the percentage of the first choice of mated females (gray, control plant; orange, beetle-infested plant). Boxplots depict median, upper, and lower quartiles. Whiskers depict quartiles ± 1.5 × the IQR. All data were included in the statistical analysis (Wilcoxon rank-sum test; binomial test, n = 10–20). *p < 0.05; **p < 0.01; ***p < 0.001. See also Figure S1.

difference (Figure S1A). In addition, *M. sexta* females showed no preference for *M. sexta*-larvae-infested plants (Figure S1B), suggesting that the recorded oviposition preference is restricted to plants damaged by *Lema*.

Previous studies have shown that oviposition by *M. quinquemaculata*[11] and *M. sexta*[12] increased significantly on *Datura* plants whose flowers had been experimentally enriched with nectar. Therefore, we asked whether flowering *Datura* would be more attractive to *M. sexta* than beetle-infested plants. To address this, we let female *M. sexta* choose between a beetle-infested plant (with beetles) and a healthy flowering plant in the wind tunnel. Strikingly, *M. sexta* significantly preferred beetle-infested plants to flowering plants (Figure S1C).

We further confirmed the results in a tent assay (Figures 1B and 1F), showing that oviposition preference for beetle-infested plants was consistent across behavioral paradigms. *M. sexta* strongly preferred beetle-infested plants.

Beetles avoid ovipositing and feeding on *M. sexta*-infested plants

Having established that *M. sexta* is attracted to beetle-infested plants, we next asked whether the beetles respond to *M. sexta*-infested plants in the same manner. Strikingly, the beetles strongly avoided ovipositing on *M. sexta*-infested plants and preferred feeding on healthy plants (Figure S1D), suggesting that beetles avoid competition with *M. sexta* larvae. Correspondingly, the dispersal of beetles to neighboring plants may be conducive to the transmission of pathogens carried by the beetles, a phenomenon that has been documented in aphids.[13]

Ionotropic receptors are not required for sensing the volatiles emitted from beetle-infested plants

It is known that *M. sexta* females choose oviposition sites based on olfactory cues employing both odorant receptor (Or)- and ionotropic receptor (Ir)-based olfaction.[14,15] To determine which olfactory pathway governs the attraction to beetle-infested plants, we tested mutant moths that lacked either Or-coreceptor (Orco), Ir8a or Ir25a. Irs are a large family of invertebrate-specific sensory receptors related to variant ionotropic glutamate receptors.[16] Ir8a and Ir25a are broadly expressed co-receptors that form heteromeric complexes with the selectively expressed Irs, which determine the sensory response specificity of the neuron.[17] Odors detected by "tuning" Irs in combination with Ir8a or Ir25a should no longer be detected in Ir8a or Ir25a

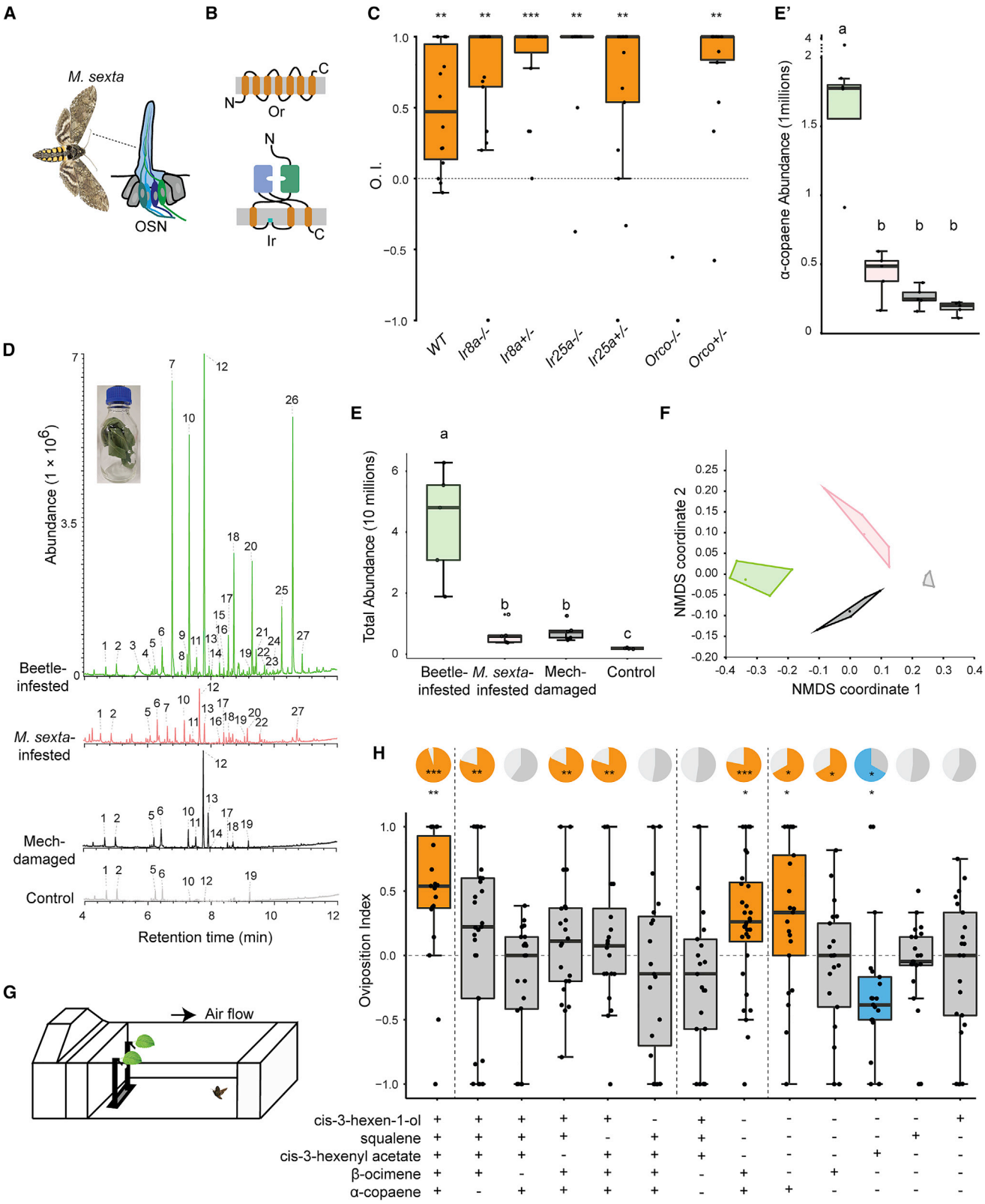

Figure 2. α-Copaene is rendering beetle-infested plants more attractive

(A) Schematic of olfactory sensory neuron (OSN) on the antenna of *M. sexta*.

(B) Protein domain organization of Ors and Irs.

(legend continued on next page)

mutants. Here, Ir8a and Ir25a mutant moths showed similar attraction to beetle-infested plants as wild-type moths, whereas Orco mutant moths were no longer attracted to beetle-infested plants, suggesting that Irs are not required for the behavioral responses to beetle-infested plants (Figure 2C) and thereby strongly implying that odors governing these responses are detected by Ors.

α-Copaene attracts oviposition in *M. sexta*

Next, to test which volatiles are responsible for this oviposition preference, we collected the headspace of leaf samples from control, mechanically damaged, *M. sexta*-infested, and beetle-infested plants and analyzed them by gas chromatography-mass spectrometry (GC-MS). We found significant qualitative and quantitative differences in volatile profiles between different treatments (Figures 2D–2F). Beetle-infested plants produced a greater variety and higher amounts of volatiles than other groups produced.

To further explore the influence of odors emitted by beetle-infested plants on *M. sexta* oviposition, we conducted a series of wind tunnel experiments with the five most abundant odors in the headspace of beetle-infested plants (odor numbers 12, 26, 7, 10, and 18 in Figure 2D) (Figure 2G). The five-odor mixture mimicked the attractiveness of beetle-infested plants to ovipositing females, whereas removing any one of the odors from the mixture rendered the remaining mixture not attractive. However, the combination of β-ocimene and α-copaene strongly induced moth approach and oviposition. Later, when we tested the moths with individual odors, α-copaene (whose emission increased significantly upon beetle infestation; Figure 2E′) alone was sufficient to elicit moth oviposition, while *cis*-3-hexenyl acetate turned out to be aversive (Figure 2H). Our results highlight the importance of blend perception in host plant recognition,[18] which seems to rely both on the proportion of the different main compounds in the blend[19] and on the integration of this information at various levels in the insect brain.[20] Our results echo with two recent studies in mice, in which some attractive and aversive odors neutralize one another's behavioral effects.[21,22] We do not rule out that other minor odors in the plant headspace may play an additional role in moth oviposition.

α-Copaene activates Or35

First, to gain insights into Ors potentially involved in detecting α-copaene, we utilized the deorphanization of receptors based on expression alterations in mRNA levels (DREAM) approach,[23] i.e., a method that takes advantage of the observation that mRNA levels of Ors change immediately after exposure to high concentrations of corresponding ligands.[24] We examined the mRNA expression levels of *Ors* and *Irs* by NanoString nCounter, a technology primarily developed for gene expression analysis.[25] We found the mRNA expression levels of four *Ors* (*Or19*, *Or26*, *Or31*, and *Or67*) and one *Ir* (*Ir8a*) decreased, while that of *Or35* increased (Figures S2A and S2B).

Next, we performed functional analysis of these Ors in *Xenopus* oocytes by recording responses using a two-electrode voltage clamp (Figure 3A). Surprisingly, given that the mRNA expression levels of *Or19*, *Or26*, and *Or67* were reduced after exposure to α-copaene, oocytes co-expressing any of these receptors (as well as the two randomly picked Or9 and Or10) and Orco showed no response to α-copaene (Figure S2C), indicating that down-regulation of chemosensory receptor expression levels following exposure is not always indicative of specific ligand-receptor interactions.[24] However, oocytes co-expressing Or35/Orco, which was upregulated in the DREAM experiment, responded robustly to α-copaene (Figures S3C and S3D). To check the specificity of Or35, we tested seven other terpenes along with α-copaene. Oocytes co-expressing Or35/Orco displayed the strongest response to α-copaene with an EC50 value of 6.406×10^{-4} M (Figures 3D and 3E) and a minor response to linalool, α-pinene, and myrcene (Figures 3B and 3C). The change in mRNA expression levels of *Ir8a* was unexpected, considering that the behavioral preference of $Ir8a^{-/-}$ mutant moths toward beetle-infested plants was not affected. However, two recent studies in fly and mosquito have found that *Ir8a* is widely expressed and co-localizes with many Ors in the antenna,[26,27] suggesting that Ir8a may interact with these Ors in some way and thus be affected in the DREAM experiments. Another possibility is that Ir8a is indeed involved in the detection of α-copaene, but in a different manner.

To get insights into where Or35 is expressed in the antennae, we utilized *in situ* hybridization. Orco, as expected, was abundantly expressed in cells visible in the longitudinal section (Figure 3G, left). Probes for Or35 labeled only one cell in each longitudinal section (Figure 3G, right), suggesting expression of Or35 in very few OSNs (chromogenic *in situ* hybridization; Figure S2E).

Next, to identify the population of OSNs that is activated by α-copaene, we performed single-sensillum recording (SSR) measurements, a method that enables us to assess odor-induced olfactory sensory neuron (OSN) activity extracellularly. In total, 39 out of 140 tested basiconic sensilla displayed responses to α-copaene and other terpenes while none of the 20 tested trichoid sensilla responded to α-copaene. Hierarchical cluster analysis identified three distinct functional OSN types. Type I OSNs showed the strongest responses to α-copaene. Type II and type III OSNs responded best to α-pinene and linalool, respectively (Figure 3H). The responses of type I OSNs

(C) O. I. in WTA of homozygous and heterozygous lines of Ir8a, Ir25a, and Orco mutants for beetle-infested versus control plants. All data were included in the statistical analysis except the $Orco^{-/-}$ as only 2 out of 19 moths oviposited. Boxplot descriptions same as in Figure 1.

(D) Representative GC-MS profile of volatiles emitted by beetle-infested, *M. sexta*-infested, mechanically damaged (Mech-damaged), and control plants. Glass bottle depicts headspace collection from leaf tissues. For identification of numbered peaks in the GC-MS chromatograms, see STAR Methods.

(E) Boxplots depict quantitative differences in all volatiles (E′, α-copaene) emitted by *Datura* with different treatments; letters indicate statistical differences (n = 5, Kruskal-Wallis).

(F) Non-metric multi-dimensional scaling (NMDS) ordination of *Datura* volatiles (one-way ANOSIM, R = 0.8437, $p < 0.0001$; Bray-Curtis dissimilarity matrix) based on 26 identified odorants.

(G) Schematic drawing of WTA with detached leaf and synthetic odors.

(H) O. I. of gravid females to various combinations of five most abundant volatiles from beetle-infested plants. Pie charts depict the percentage of the first choice (light gray, control leaf; dark gray, scented leaf; orange, significant attraction; blue, significant aversion; binomial test, n = 17–32). Boxplot descriptions same as in Figure 1.

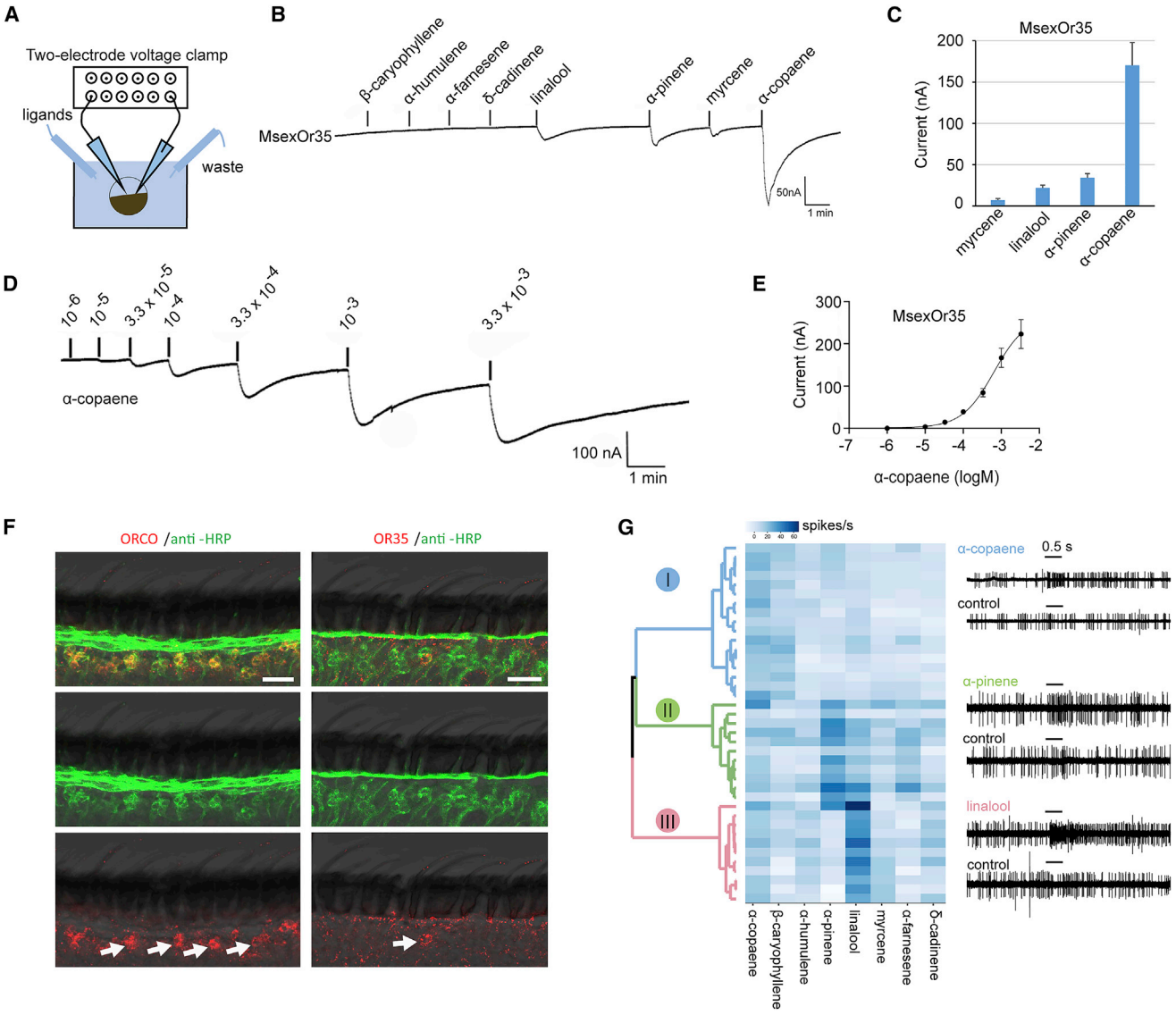

Figure 3. α-Copaene activates Or35

(A) Schematic drawing of two-electrode voltage-clamp recording.

(B and C) Representative recording traces of inward current responses (B) and response profiles (C) of *Xenopus* oocytes co-expressing MsexOr35/MsexOrco stimulated by a range of compounds. Error bars indicate SEM (n = 10).

(D) Inward current responses of *Xenopus* oocytes co-expressing MsexOr35/MsexOrco stimulated by α-copaene at a range of concentrations.

(E) Dose-response curve for MsexOr35/MsexOrco-expressing *Xenopus* oocytes treated with α-copaene.

(F) Visualization of Orco or Or35-expressing cells from a female antenna. FISH with an antisense riboprobe for Orco (left) (red) and Or35 (right) (red) on longitudinal sections through antennae that were counterstained with anti-HRP (green). The green coloring of the cuticle is based on autofluorescence. Hybridization signals are denoted by arrows. Scale bars, 20 μm.

(G) Left: hierarchical cluster analysis of 39 basiconic sensilla, tested with 8 odorants. Dendrogram (based on Ward's method in R): horizontal rows represent 39 sensilla and vertical columns represent 8 odorants. Baseline activity and response to solvent (DMSO) have been subtracted. Sensillum type I, n = 17; type II, n = 11; type III, n = 11. Right: representative SSR traces of each basiconic sensillum type to the best ligand.

See also Figure S2.

resemble the responses of Or35 in the oocyte, except that type I OSNs additionally respond to β-caryophyllene. This discrepancy could be explained by the lack of odorant-binding proteins (OBPs) in the oocyte system, which has been demonstrated previously.[28] Together, while DREAM indeed provided a valuable prediction of Or35, though, among several false-positive results, our SSR result highlights potential false-negative results from this method, as additional receptors not identified by DREAM respond to α-copaene. Therefore, DREAM predictions should always be verified *in vitro* and *in vivo*.[24]

Beetle infestation suppresses plant defense

A previous study reported that Colorado potato beetle larvae secrete symbiotic bacteria to plant wounds to suppress plant

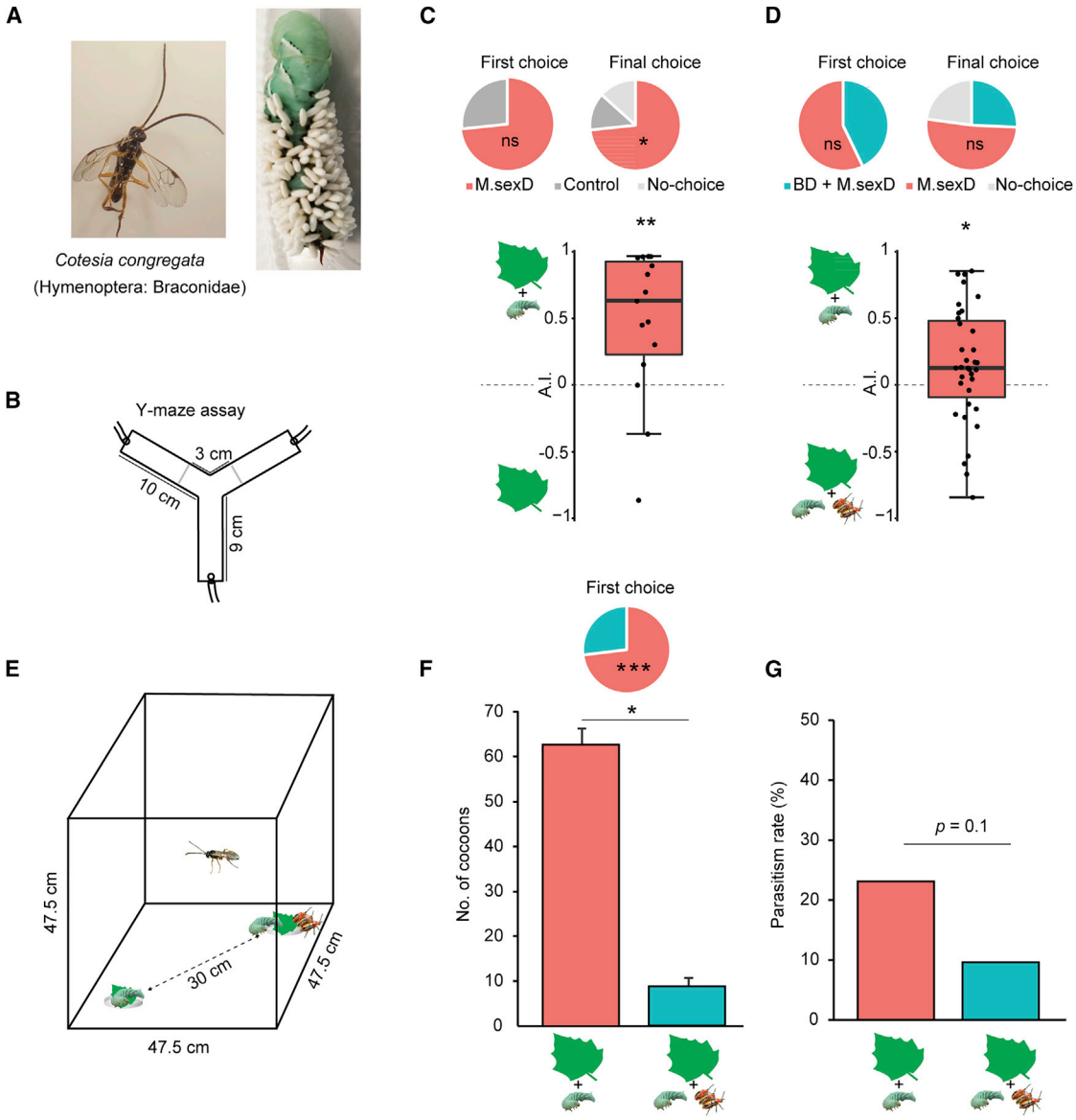

Figure 4. Beetle-infested plants confer protection against endoparasitoid wasps

(A) Endoparasitoid wasp *C. congregata* and its pupae attached to *M. sexta* larva.

(B) Schematic drawing of Y maze assay.

(C) First choice, final choice, and attraction index (A. I. = (time in treatment − time in control)/total time) for Y maze arm with headspace from *M. sexta*-infested (M.sexD) versus control plant (n = 15).

(D) Same analysis as (C), but with *M. sexta*-infested tested versus *M. sexta*- and beetle-infested plant (BD) (n = 35) (Wilcoxon rank-sum test; deviation against even distribution was tested by binomial test). Boxplot descriptions same as in Figure 1.

(E) Tent assay.

(F) Bar plot depicts mean numbers of *Cotesia* cocoons that emerged from *Manduca* caterpillars (n = 17, Mann-Whitney U test, *p < 0.05); whiskers depict standard error. The pie chart depicts the ratio of the first choice of wasps toward M.sexD or BD. Deviation against even distribution was tested by binomial test. *p < 0.05. Wasps that did not choose were excluded from statistical analysis.

(G) The death rate, rate of caterpillars killed by *Cotesia* on M.sexD and BD plants (n = 52, chi-square test). For plant defenses and nutrient analysis, see Figures S3 and S4.

defenses, which then leads to enhanced growth of the offspring.[29] Here, we checked whether plant defenses were weakened following beetle infestation. We first qualitatively examined the chemical constituents of beetle-infested, *M. sexta*-infested, and control plants via HPLC-timsTOF measurements. The PCA of the obtained data revealed a clear separation of these three groups (Figure S3A). We then quantified the well-described chemical defense compounds in *Datura*, atropine and (-)-scopolamine.[30] Interestingly, the levels of both atropine and (-)-scopolamine were significantly reduced in

beetle-infested plants as compared with *M. sexta*-infested and control plants, suggesting that beetle infestation suppressed these chemical defenses of the plant (Figures S3B and S3C).

M. sexta larvae perform worse on beetle-infested plants

Next, we asked whether compromised plant defenses provide any fitness benefits for the caterpillars that develop on beetle-infested plants. We reared *M. sexta* larvae on control, beetle-infested leaf disks, and artificial diet as well as on intact plants (control and beetle-infested plants) for 1 week starting from neonate larvae. Caterpillars that were reared on beetle-infested plants/leaf disks gained less mass and grew more slowly over time than those reared on control plants/leaf disks or artificial diet (Figures S3D and S3E). When reared on beetle-infested plants, the weight of *M. sexta* pupae was comparable to those reared on control plants (Figure S3F), although the former pupated 4–5 days later (data not shown). The reduced levels of alkaloids in beetle-infested plants thus did not result in a direct fitness advantage for *M. sexta* caterpillars. We then analyzed the nutrients in beetle-infested and control plants, as well as in caterpillars. Interestingly, 16 out of the 18 analyzed amino acids were considerably increased in beetle-infested plants compared with control (Figure S3G). Asparagine and threonine in caterpillars fed on beetle-infested plants increased while histidine decreased compared with caterpillars fed on control plants (Figure S3H). Sucrose decreased in beetle-infested plants compared with control plants (Figure S3I), while fructose in caterpillars fed on beetle-infested plants increased compared with caterpillars fed on control plants (Figure S3J). To test whether the extremely high concentration of threonine in caterpillars explains the impaired performance observed, we coated *Datura* leaf disks with threonine. Glutamine was added as a positive control. Notably, caterpillars performed the worst when threonine was supplemented. Glutamine supplementation did not affect the growth of caterpillars compared with the control (Figures S3K and S3L). Therefore, plant defense and nutrients could not provide an adaptive explanation for the moths' enigmatic oviposition preference.

Beetle-infested plants may confer protection against endoparasitoid wasps

Next, we asked whether the parasitoid wasp *C. congregata* is the reason for the moths' oviposition preference. Parasitism rates of *C. congregata* (Figure 4A) on *M. sexta* may reach 50%–90% in the southeastern USA.[31,32] The wasps thus constitute an extremely important selection pressure because being parasitized typically leads to the death of the caterpillar. We investigated the preferences of *C. congregata* in Y maze experiments (Figure 4B). First, we offered wasps a choice between control and *M. sexta*-infested plants. Although no difference was found concerning the first choice, significantly more wasps ended up in the arm containing the odor of *M. sexta*-infested plants and spent more time exploring it (Figure 4C). When the odor of *M. sexta*-infested plants was contrasted against the odor of *M. sexta*-beetle-infested plants, wasps showed a preference for the *M. sexta*-infested plants (Figure 4D), suggesting that wasps avoid the scents emitted from *M. sexta*-beetle-infested plants. We further verified wasps' behavior in a tent (Figure 4E). When wasps had the choice to oviposit on caterpillars that were feeding on a plant in either presence or absence of the beetles, the wasps were not only less attracted to *M. sexta*-beetle-infested plants but also showed poorer performance (Figure 4F), suggesting that *M. sexta* feeding on beetle-infested plants may not be suitable for the development of wasp larvae. Both these results likely contributed to the trend that a higher parasitism (i.e., death) rate (23% without beetles versus 9% with beetles) was observed in caterpillars feeding in the absence of protecting beetles (Figure 4G).

Previous studies have shown some ecological trade-offs, where ovipositing tobacco hawkmoths prefer *Proboscidea* over *Datura* plants despite *Proboscidea*'s inferior nutritional quality. The moths' preference may be attributed to the hairy structure of *Proboscidea* leaves protecting *M. sexta* caterpillars against parasitism.[33,34] Also, the diamondback moth *Plutella xylostella* prefers to oviposit on cabbage plants that were already damaged by *Pieris rapae* larvae, though this might expose their offspring to some challenges.[4,35] A recent finding showed that female brown planthoppers preferentially oviposit on rice plants that have been infested by the rice striped stem borer, despite the potential competition arising from the dual attack.[5] These, at first glance, "poor" female oviposition choices led to reduced parasitism rates in the offspring.[8,19,34] Therefore, it is tempting to propose that *M. sexta* females make a trade-off during oviposition and to some extent sacrifice the growth rate of their offspring for lower parasitism rates by ovipositing on beetle-infested plants. Our study sheds light on the molecular and olfactory mechanisms behind this trade-off.

STAR★METHODS

Detailed methods are provided in the online version of this paper and include the following:

- KEY RESOURCES TABLE
- RESOURCE AVAILABILITY
  - Lead Contact
  - Materials Availability
  - Data and Code Availability
- EXPERIMENTAL MODEL AND SUBJECT DETAILS
  - Animals and Plants
- METHOD DETAILS
  - *M. sexta* Behavioral Test
  - Beetle Choice Assay
  - Performance of *M. sexta* Larvae
  - Volatile Chemical Analysis
  - Non-volatile Chemical Analysis
  - Caterpillar Fitness With Enhanced Amino Acid Concentrations
  - Parasitoid Wasp Y-maze Assays
  - Parasitoid Wasp Tent Assays
  - Generation of Antisense Riboprobes for In Situ Hybridization
  - In Situ Hybridization
  - Single Sensillum Recording (SSR)
  - Odorant Exposure, Tissue Collection, and RNA Extraction
  - Nanostring Assay
  - Gene Cloning

- Vector Construction and cRNA Synthesis
- Receptor Expression in *Xenopus* Oocytes and Two Electrode Voltage Clamp Electrophysiological Recordings

- QUANTIFICATION AND STATISTICAL ANALYSIS

SUPPLEMENTAL INFORMATION

Supplemental information can be found online at https://doi.org/10.1016/j.cub.2021.12.021.

ACKNOWLEDGMENTS

We thank Sascha Bucks for *Manduca* rearing, Kerstin Weniger for assistance in chemical analysis, Jürgen Krieger for his valuable input at *in situ* hybridization, Danny Kessler for providing *Lema* beetles, and the greenhouse team for providing plants. This research was supported through funding by the Max Planck Society and the Alexander von Humboldt Foundation.

AUTHOR CONTRIBUTIONS

J.Z. conceptualized and designed the project with M.K. and B.S.H. All authors contributed to the experimental design, analysis, and interpretation of results. J.Z. prepared all figures. Experimental contributions were as follows: J.Z. (Figures 1, 2, 3H, 4C, S2A, S2B, S3D, S3E, S4E, and S4F), S.A.K.R. (Figures 2H, 4D, 4F, and S1), Z.W. (Figures 3B–3E), I.W.K. (Figure 2D), A.L.P. (Figure 4D), F.F. (Figures S3A–S3C), J.C. (Figures S3A–S3D), S.C. (Figures 3F and S2E), and R.A.F. and E.G.-W. (Figure S2). J.Z. wrote the original manuscript, and M.K. and B.S.H. contributed to the final manuscript. All co-authors contributed to the subsequent revisions.

DECLARATION OF INTERESTS

The authors declare no competing interests.

Received: August 1, 2021
Revised: October 27, 2021
Accepted: December 8, 2021
Published: January 10, 2022

REFERENCES

1. Poelman, E.H. (2015). From induced resistance to defence in plant-insect interactions. Entomol. Exp. Appl. *157*, 11–17.
2. Aljbory, Z., and Chen, M.-S. (2018). Indirect plant defense against insect herbivores: a review. Insect Sci *25*, 2–23.
3. Mithöfer, A., and Boland, W. (2012). Plant defense against herbivores: chemical aspects. Annu. Rev. Plant Biol. *63*, 431–450.
4. Shiojiri, K., Takabayashi, J., Yano, S., and Takafuji, A. (2002). Oviposition preferences of herbivores are affected by tritrophic interaction webs. Ecol. Lett. *5*, 186–192.
5. Hu, X.Y., Su, S.L., Liu, Q.S., Jiao, Y.Y., Peng, Y.F., Li, Y.H., and Turlings, T.C.J. (2020). Caterpillar-induced rice volatiles provide enemy-free space for the offspring of the brown planthopper. eLife *9*, 19.
6. Hare, J.D., and Elle, E. (2002). Variable impact of diverse insect herbivores on dimorphic *Datura wrightii*. Ecology *83*, 2711–2720.
7. Hare, J.D. (2007). Variation in herbivore and methyl jasmonate-induced volatiles among genetic lines of *Datura wrightii*. J. Chem. Ecol. *33*, 2028–2043.
8. Goldberg, J.K., Sternlieb, S.R., Pintel, G., and Delph, L.F. (2021). Observational evidence of herbivore-specific associational effects between neighboring conspecifics in natural, dimorphic populations of *Datura wrightii*. Ecol. Evol. *11*, 5547–5561.
9. Morton, T.C., and Vencl, F.V. (1998). Larval beetles form a defense from recycled host-plant chemicals discharged as fecal wastes. J. Chem. Ecol. *24*, 765–785.
10. Hare, J.D., and Sun, J.J. (2011). Production of induced volatiles by *Datura wrightii* in response to damage by insects: effect of herbivore species and time. J. Chem. Ecol. *37*, 751–764.
11. Kessler, D. (2012). Context dependency of nectar reward-guided oviposition. Entomol. Exp. Appl. *144*, 112–122.
12. Adler, L.S., and Bronstein, J.L. (2004). Attracting antagonists: does floral nectar increase leaf herbivory? Ecology *85*, 1519–1526.
13. Mauck, K.E., De Moraes, C.M., and Mescher, M.C. (2010). Deceptive chemical signals induced by a plant virus attract insect vectors to inferior hosts. Proc. Natl. Acad. Sci. USA *107*, 3600–3605.
14. Zhang, J., Bisch-Knaden, S., Fandino, R.A., Yan, S.W., Obiero, G.F., Grosse-Wilde, E., Hansson, B.S., and Knaden, M. (2019). The olfactory coreceptor IR8a governs larval feces-mediated competition avoidance in a hawkmoth. Proc. Natl. Acad. Sci. USA *116*, 21828–21833.
15. Fandino, R.A., Haverkamp, A., Bisch-Knaden, S., Zhang, J., Bucks, S., Nguyen, T.A.T., Schröder, K., Werckenthin, A., Rybak, J., Stengl, M., et al. (2019). Mutagenesis of odorant coreceptor *Orco* fully disrupts foraging but not oviposition behaviors in the hawkmoth *Manduca sexta*. Proc. Natl. Acad. Sci. USA *116*, 15677–15685.
16. Croset, V., Rytz, R., Cummins, S.F., Budd, A., Brawand, D., Kaessmann, H., Gibson, T.J., and Benton, R. (2010). Ancient protostome origin of chemosensory ionotropic glutamate receptors and the evolution of insect taste and olfaction. PLoS Genet *6*, e1001064.
17. Abuin, L., Bargeton, B., Ulbrich, M.H., Isacoff, E.Y., Kellenberger, S., and Benton, R. (2011). Functional architecture of olfactory ionotropic glutamate receptors. Neuron *69*, 44–60.
18. Bruce, T.J., and Pickett, J.A. (2011). Perception of plant volatile blends by herbivorous insects—finding the right mix. Phytochemistry *72*, 1605–1611.
19. Conchou, L., Lucas, P., Meslin, C., Proffit, M., Staudt, M., and Renou, M. (2019). Insect odorscapes: from plant volatiles to natural olfactory scenes. Front. Physiol. *10*, 972.
20. Galizia, C.G. (2014). Olfactory coding in the insect brain: data and conjectures. Eur. J. Neurosci. *39*, 1784–1795.
21. Saraiva, L.R., Kondoh, K., Ye, X., Yoon, K.-H., Hernandez, M., and Buck, L.B. (2016). Combinatorial effects of odorants on mouse behavior. Proc. Natl. Acad. Sci. USA *113*, E3300–E3306.
22. Qiu, Q., Wu, Y., Ma, L., and Yu, C.R. (2021). Encoding innately recognized odors via a generalized population code. Curr. Biol. *31*, 1813–1825, e4.
23. von der Weid, B., Rossier, D., Lindup, M., Tuberosa, J., Widmer, A., Col, J.D., Kan, C., Carleton, A., and Rodriguez, I. (2015). Large-scale transcriptional profiling of chemosensory neurons identifies receptor-ligand pairs *in vivo*. Nat. Neurosci. *18*, 1455–1463.
24. Koerte, S., Keesey, I.W., Khallaf, M.A., Cortés Llorca, L., Grosse-Wilde, E., Hansson, B.S., and Knaden, M. (2018). Evaluation of the DREAM technique for a high-throughput deorphanization of chemosensory receptors in *Drosophila*. Front. Mol. Neurosci. *11*, 366.
25. Goytain, A., and Ng, T. (2020). NanoString nCounter technology: high-throughput RNA validation. Methods Mol. Biol. *2079*, 125–139.
26. Younger, M.A., Herre, M., Ehrlich, A.R., Gong, Z., Gilbert, Z.N., Rahiel, S., Matthews, B.J., and Vosshall, L.B. (2020). Non-canonical odor coding ensures unbreakable mosquito attraction to humans. bioRxiv. https://doi.org/10.1101/2020.1111.1107.368720.
27. Task, D., Lin, C.-C., Afify, A., Li, H., Vulpe, A., Menuz, K., and Potter, C.J. (2020). Widespread polymodal chemosensory receptor expression in *Drosophila* olfactory neurons. bioRxiv. https://doi.org/10.1101/2020.1111.1107.355651.
28. Xu, P., Atkinson, R., Jones, D.N.M., and Smith, D.P. (2005). *Drosophila* OBP LUSH is required for activity of pheromone-sensitive neurons. Neuron *45*, 193–200.

29. Chung, S.H., Rosa, C., Scully, E.D., Peiffer, M., Tooker, J.F., Hoover, K., Luthe, D.S., and Felton, G.W. (2013). Herbivore exploits orally secreted bacteria to suppress plant defenses. Proc. Natl. Acad. Sci. USA *110*, 15728–15733.

30. Castillo, G., Cruz, L.L., Tapia-López, R., Olmedo-Vicente, E., Carmona, D., Anaya-Lang, A.L., Fornoni, J., Andraca-Gómez, G., Valverde, P.L., and Núñez-Farfán, J. (2014). Selection mosaic exerted by specialist and generalist herbivores on chemical and physical defense of *Datura stramonium*. PLoS One *9*, e102478.

31. Kester, K.M., and Barbosa, P. (1991). Behavioral and ecological constraints imposed by plants on insect parasitoids: implications for biological control. Biol. Control *1*, 94–106.

32. Kester, K.M., and Barbosa, P. (1994). Behavioral responses to host foodplants of two populations of the insect parasitoid *Cotesia congregata* (Say). Oecologia *99*, 151–157.

33. Mira, A., and Bernays, E.A. (2002). Trade-offs in host use by *Manduca sexta*: plant characters vs natural enemies. Oikos *97*, 387–397.

34. Garvey, M.A., Creighton, J.C., and Kaplan, I. (2020). Tritrophic interactions reinforce a negative preference-performance relationship in the tobacco hornworm (*Manduca sexta*). Ecol. Entomol. *45*, 783–794.

35. Shiojiri, K., Takabayashi, J., Yano, S., and Takafuji, A. (2001). Infochemically mediated tritrophic interaction webs on cabbage plants. Popul. Ecol. *43*, 23–29.

36. Koenig, C., Hirsh, A., Bucks, S., Klinner, C., Vogel, H., Shukla, A., Mansfield, J.H., Morton, B., Hansson, B.S., and Grosse-Wilde, E. (2015). A reference gene set for chemosensory receptor genes of *Manduca sexta*. Insect Biochem. Mol. Biol. *66*, 51–63.

37. Haverkamp, A., Bing, J., Badeke, E., Hansson, B.S., and Knaden, M. (2016). Innate olfactory preferences for flowers matching proboscis length ensure optimal energy gain in a hawkmoth. Nat. Commun. *7*, 11644.

38. Crocoll, C., Mirza, N., Reichelt, M., Gershenzon, J., and Halkier, B.A. (2016). Optimization of engineered production of the glucoraphanin precursor dihomomethionine in *Nicotiana benthamiana*. Front. Bioeng. Biotechnol. *4*, 14.

39. Lackner, S., Lackus, N.D., Paetz, C., Köllner, T.G., and Unsicker, S.B. (2019). Aboveground phytochemical responses to belowground herbivory in poplar trees and the consequence for leaf herbivore preference. Plant Cell Environ *42*, 3293–3307.

40. Wei, J.-N., and Kang, L. (2006). Electrophysiological and behavioral responses of a parasitic wasp to plant volatiles induced by two leaf miner species. Chem. Senses *31*, 467–477.

41. Pregitzer, P., Jiang, X., Grosse-Wilde, E., Breer, H., Krieger, J., and Fleischer, J. (2017). In search for pheromone receptors: certain members of the odorant receptor family in the desert locust *Schistocerca gregaria* (Orthoptera: Acrididae) are co-expressed with SNMP1. Int. J. Biol. Sci. *13*, 911–922.

42. Fleischer, J., Rausch, A., Dietze, K., Erler, S., Cassau, S., and Krieger, J. (2021). A small number of male-biased candidate pheromone receptors are expressed in large subsets of the olfactory sensory neurons in the antennae of drones from the European honey bee *Apis mellifera*. Insect Sci. Published online *August 4*, 2021. https://doi.org/10.1111/1744-7917.12960.

43. Sun, B., and Salvaterra, P.M. (1995). Characterization of nervana, a *Drosophila melanogaster* neuron-specific glycoprotein antigen recognized by anti-horseradish peroxidase antibodies. J. Neurochem. *65*, 434–443.

44. Ghaninia, M., Olsson, S.B., and Hansson, B.S. (2014). Physiological organization and topographic mapping of the antennal olfactory sensory neurons in female hawkmoths. *Manduca sexta*. Chem. Senses *39*, 655–671.

45. Shanbhag, S.R., Müller, B., and Steinbrecht, R.A. (1999). Atlas of olfactory organs of *Drosophila melanogaster*: 1. Types, external organization, innervation and distribution of olfactory sensilla. Int. J. Insect Morphol. Embryol. *28*, 377–397.

46. Shields, V.D.C., and Hildebrand, J.G. (2001). Recent advances in insect olfaction, specifically regarding the morphology and sensory physiology of antennal sensilla of the female sphinx moth *Manduca sexta*. Microsc. Res. Tech. *55*, 307–329.

47. Yao, C.A., Ignell, R., and Carlson, J.R. (2005). Chemosensory coding by neurons in the coeloconic sensilla of the *Drosophila* antenna. J. Neurosci. *25*, 8359–8367.

48. Silbering, A.F., Rytz, R., Grosjean, Y., Abuin, L., Ramdya, P., Jefferis, G.S.X.E., and Benton, R. (2011). Complementary function and integrated wiring of the evolutionarily distinct *Drosophila* olfactory subsystems. J. Neurosci. *31*, 13357–13375.

49. Guo, J.-M., Liu, X.-L., Liu, S.-R., Wei, Z.-Q., Han, W.-K., Guo, Y., and Dong, S.-L. (2020). Functional characterization of sex pheromone receptors in the Fall armyworm (*Spodoptera frugiperda*). Insects *11*, 193.

STAR★METHODS

KEY RESOURCES TABLE

REAGENT or RESOURCE	SOURCE	IDENTIFIER
Antibodies		
goat-anti-HRP Alexa Fluor 647-conjugated antibody	Jackson ImmunoResearch, Ely, Great Britain	Cat#123-605-021; RRID: AB_2338967
Chemicals, peptides, and recombinant proteins		
3-hexanone	Sigma-Aldrich	589-38-8
2-hexanone	Sigma-Aldrich	591-78-6
3-hexenal	Sigma-Aldrich	6789-80-6
2-heptanone	Fluka	110-43-0
3-hexanol	Sigma-Aldrich	623-37-0
(*E*)-2-hexenal	Fluka	6728-26-3
β-ocimene	Sigma-Aldrich	13877-91-3
methyl heptanoate	Sigma-Aldrich	106-73-0
tridecane	Merck	629-50-5
cis-3-hexenyl acetate	Sigma-Aldrich	3681-71-8
1-hexanol	Fluka	111-27-3
cis-3-hexen-1-ol	Sigma-Aldrich	928-96-1
cis-2-hexen-1-ol	Sigma-Aldrich	928-94-9
tetradecane	Sigma-Aldrich	629-59-4
1-octen-3-ol	Merck	3391-86-4
trans-3-hexenyl butyrate	Toronto Research Chemicals	53398-84-8
2-ethyl-1-hexanol	Fluka	104-76-7
α-copaene	Toronto Research Chemicals	3856-25-5
1-bromodecane	Sigma-Aldrich	112-29-8
trans-α-bergamotene	Toronto Research Chemicals	17829-53-7
β-caryophyllene	Fluka	87-44-5
cis-3-hexenyl hexanoate	Sigma-Aldrich	31501-11-8
cis-3-hexenyl lactate	Sigma-Aldrich	61931-81-5
α-farnesene	Sigma-Aldrich	502-61-4
squalene	Sigma-Aldrich	111-02-4
benzyl alcohol	Fluka	100-51-6
α-humulene	Sigma-Aldrich	6753-98-6
α-pinene	Sigma-Aldrich	80-56-8
linalool	Sigma-Aldrich	78-70-6
myrcene	Fluka	123-35-3
δ-cadinen	Boc sciences	483-76-1
dimethyl sulfoxide	Sigma-Aldrich	67-68-5
Oligonucleotides		
Msor19F	Genscript Biotech	5'-ATGACATCCCACGTT ACTGC-3'
Msor19R	Genscript Biotech	5'-TTATCCCTCGTTGGCTTGT-3'
Msor26F	Genscript Biotech	5'-ATGGCAAGCTACGAAGGAA-3'
Msor26R	Genscript Biotech	5'-TCAATATAAAAGCGAAAGC ACT-3'
Msor31F	Genscript Biotech	5'-ATGGCTCAAAACACAGA ATTATT-3'

(*Continued on next page*)

Continued

REAGENT or RESOURCE	SOURCE	IDENTIFIER
Msor31R	Genscript Biotech	5'-TTATGTGTTCGCCCTGT TGA-3'
Msor35F	Genscript Biotech	5'-ATGGTTGTCATAGAGAAA ATTTTAA-3'
Msor35R	Genscript Biotech	5'-TTAATTTGTTCCTTTTAAT AATGTGTA-3'
Msor67F	Genscript Biotech	5'-ATGCGGCCAACGCGTTAT-3'
Msor67R	Genscript Biotech	5'-TTACACTTGGACCTCCTTT TGGC-3'
MscoF	Genscript Biotech	5'-ATGATGGCCAAAGTGAAA AC-3'
MscoR	Genscript Biotech	5'-CTATTTCAGCTGCACCAA CAC-3'
Msor9F	Genscript Biotech	5'-ATGACATCCCCTGACAGCA-3'
Msor9R	Genscript Biotech	5'-TTAGTACAGGAGCGAGAA TATTGA-3'
Msor10F	Genscript Biotech	5'-ATGGCGCTTCAATTCGAC-3'
Msor10R	Genscript Biotech	5'-TTATTGACCGTACACCGT TTG-3'
Msor19F-EcoRI-F	Genscript Biotech	5'-ATTCCCCGGGGATCC **GAATTC**ATGACATCCCAC GTTACTGC-3'
Msor19-XbaI-R	Genscript Biotech	5'-TCGGCGATCGGGCCC**TCTAGA** TTATCCCTCGTTGGCTTGT-3'
Msor26-EcoRI-F	Genscript Biotech	5'-ATTCCCCGGGGATCC**GAATTC** ATGGCAAGCTACGAAGGAA-3'
Msor26-XbaI-R	Genscript Biotech	5'-TCGGCGATCGGGCCC **TCTAGA**TCAATATAAAAG CGAAAGCACT-3'
Msor35-EcoRI-F	Genscript Biotech	5'-ATTCCCCGGGGATCC **GAATTC**ATGGTTGTCATA GAGAAAATTTTAA-3'
Msor35-XbaI-R	Genscript Biotech	5'-TCGGCGATCGGGCCC **TCTAGA**TTAATTTGTTCCT TTTAATAATGTGTA-3'
Msor67-EcoRI-F	Genscript Biotech	5'-ATTCCCCGGGGATCC **GAATTC**ATGCGGCCAAC GCGTTAT-3'
Msor67-XbaI-R	Genscript Biotech	5'-TCGGCGATCGGGCCC **TCTAGA**TTACACTTGGAC CTCCTTTTGGC-3'
Msco-EcoRI-F	Genscript Biotech	5'-ATTCCCCGGGGATCC **GAATTC**ATGATGGCCAA AGTGAAAAC-3'
Msco-XbaI-R	Genscript Biotech	5'-TCGGCGATCGGGCCC **TCTAGA**CTATTTCAGCTG CACCAACAC-3'
Msor9-EcoRI-F	Genscript Biotech	5'-ATTCCCCGGGGATCC **GAATTC**ATGACATCCCC TGACAGCA-3'
Msor9-XbaI-R	Genscript Biotech	5'-TCGGCGATCGGGCCC **TCTAGA**TTAGTACAGGAG CGAGAATATTGA-3'
Msor10-EcoRI-F	Genscript Biotech	5'-ATTCCCCGGGGATCC **GAATTC**ATGGCGCTTCA ATTCGAC-3'

(*Continued on next page*)

Continued

REAGENT or RESOURCE	SOURCE	IDENTIFIER
Msor10-XbaI-R	Genscript Biotech	5'-TCGGCGATCGGGCCC **TCTAGA**TTATTGACCGTA CACCGTTTG-3'
MscoF-in situ	Eurofins	5'-ATGATGGCCAAAGTGAA AAC-3'
MscoR-in situ	Eurofins	5'-CTATTTCAGCTGCACCA ACAC-3'
Msor35F-in situ	Eurofins	5'-CACCGATGATCTCAAATT GATT-3'
Msor35R-in situ	Eurofins	5'-ACTTCCTTCTGTATGTTC TTGT-3'
Software, algorithms, and instruments		
MetaboAnalyst 5.0	https://www.metaboanalyst.ca	Version 5.0
Adobe Illustrator	https://www.adobe.com/products/illustrator.html	Version CS5
PAST	https://www.nhm.uio.no/english/research/infrastructure/past/	Version 3.25
Rstudio	https://www.rstudio.com/products/rstudio/download/	Version 1.3.1093
R	https://cran.r-project.org/src/base/R-3/	Version 3.5.1
MetaboScape	Bruker Daltonik	https://www.bruker.com/en/products-and-solutions/mass-spectrometry/ms-software/metaboscape.html
Two-electrode voltage-clamp	Warner Instruments	RC-3Z/OC-725C
Axon pCLAMP	Axon Instruments, Union City, CA, USA	Version 8.2
nSolver Analysis Software	NanoString Technologies, Seattle, WA, USA	version 4.0
NanoDrop	Thermo Fisher Scientific, Waltham, MA, USA	https://www.thermofisher.com/order/catalog/product/de/en/ND-ONE-W
confocal LSM 880 laser scanning microscope	Carl Zeiss, Germany	https://www.zeiss.com/microscopy/us/products/confocal-microscopes.html#more
Leica DMLB microscope	Leica Microsystems, Wetzlar, Germany	https://www.leica-microsystems.com/
Canon EOS 700D camera	Canon, Tokyo, Japan	N/A
QTRAP 6500+ triple quadrupole mass spectrometer	AB Sciex LLC, Framingham, MA, USA	https://sciex.com/products/mass-spectrometers/qtrap-systems/qtrap-6500-system
Dionex Ultimate 3000 series UHPLC	Thermo Fisher Scientific, Waltham, MA, USA	https://www.thermofisher.com/de/en/home.html
GC-MS	Agilent, USA	Agilent 6890 GC & 5975C MS
Other		
pEASY-Blunt3 cloning kit	TransGenBiotech Beijing	CB301-02
mMESSAGE mMACHINE T7 Kit	Thermo Fisher Scientific, Waltham, MA, USA	https://www.thermofisher.com/order/catalog/product/AM1344
ClonExpress Ultra One Step Cloning Kit	Vazyme, Nanjing, China	https://www.vazymebiotech.com/product/83.html
AxyPrep DNA Gel Extraction Kit	Axygen, Suzhou, China	https://www.selectscience.net/products/axyprep-dna-gel-extraction-kit/?prodID=83583
Trans1-T1 Phage Resistant Chemically Competent Cells	TransGen Biotech, Beijing, China	https://www.globalsources.com/si/AS/Beijing-Transgen/6008847592915/pdtl/Trans1-T1-Phage-Resistent-Chemically-Competent-Cell/1078397963.htm

(*Continued on next page*)

Continued

REAGENT or RESOURCE	SOURCE	IDENTIFIER
RNA isolation kit	ZYMO research	https://www.zymoresearch.de/products/direct-zol-rna-miniprep-kits
TOPO TA Cloning Vector	ThermoFisher, Waltham, Massachusetts, USA	https://www.thermofisher.com/order/catalog/product/K4575J10

RESOURCE AVAILABILITY

Lead Contact

Further information and requests for resources should be directed to and will be fulfilled by the Lead Contact, (mknaden@ice.mpg.de).

Materials Availability

This study did not generate new unique reagents.

Data and Code Availability

- All data reported in this paper will be shared by the lead contact upon request.
- This paper does not report original code.
- Any additional information required to reanalyze the data reported in this paper is available from the lead contact upon request.

EXPERIMENTAL MODEL AND SUBJECT DETAILS

Animals and Plants

M. sexta, which originally came from Arizona, were reared at the Max Planck Institute for Chemical Ecology, Jena, Germany, as already described.[36] Briefly, eggs were collected from female *M. sexta* moths, which could freely oviposit on *Datura* plants. Larvae used in the experiments were reared on an artificial diet, under 16:8 h light: dark photoperiod with a relative humidity of 40% at 26°C. Naïve females were mated the second night after emergence and tested during the subsequent night. Orco, Ir8a and Ir25a mutant moths were generated through CRISPR/Cas9 in the lab and kept separately from the wild-type colony but under the same conditions.[14,15] All plants were grown in a greenhouse as described.[37] Plants used for experiments were not yet flowering. Approximately 7 days before being used, plants were transferred into a climate chamber with the same settings as the moth flight cage (16:8 h light: dark photoperiod with a relative humidity of 40% at 26°C). *Lema* beetles were originally collected from the field of Utah (USA) and reared on *Datura* plants under a 16:8 h light: dark photoperiod with a relative humidity of 40% at 26°C in the lab. *Cotesia* wasps were obtained from the lab colony maintained at the University of North Carolina, Chapel Hill, North Carolina, USA. Wasps were originally sourced from *M. sexta caterpillars* collected in 2005 from the Southern Piedmont Agricultural Research and Experimental Station (Blackstone, Nottoway Co. site; 37.0817◦N, 77.9755◦W). Adult wasps were fed a 60% honey-agar solution and provided with damp sponges for water. Cocoons and adult wasps were maintained at 26°C.

METHOD DETAILS

M. sexta Behavioral Test

To investigate how gravid female *M. sexta* respond to beetle-damaged plants, we performed a two-choice assay in a transparent wind tunnel (220 × 90 × 90 cm^3) at 25 °C, 70% relative humidity, 0.3 lux illumination, and a wind speed of 40 cm/s. Treated and control *Datura* plants were placed at the upwind end of the wind tunnel. For the treated plants, 10 third instar *Lema* larvae or 10 *Lema* adults were placed on each plant and were allowed to feed for 3 days. The control plants were healthy plants of similar size. As described before,[14] mated female moths were released at the downwind side of the wind tunnel and during 3 min were allowed to oviposit on both plants. Afterwards, we counted the number of eggs on each plant. For the experiment with adults removed, the *Datura* plants were treated as abovementioned; however, we removed the adults before the wind tunnel test. The synthetic odor screen experiment was performed according to Zhang et al.[14] Two freshly detached leaves of similar size were presented to a gravid female. Each leaf was attached to the tip of one of 2 upright acrylic glass poles (40 cm high and placed at the upwind end of the wind tunnel with a distance of 40 cm between them). Beneath each leaf, we attached a square filter paper (2 × 2 cm^2) loaded with 10 μl of diluted odorant (1:10^2) or the solvent (mineral oil) alone. Moths, leaves, and filter papers were tested only once.

In addition to the wind tunnel, we also performed an oviposition assay in a tent (180 × 180 × 180 cm^3, white fine polyester mesh). Treated and control *Datura* plants were placed diagonally with a distance of 2 meters. The positions of treatment and control plants

were swapped after every second moth. Moths and plants were used only once. The oviposition index was calculated as (T-C)/(T+C) where T is the number of eggs on the treatment site and C is the number of eggs on the control site.

Beetle Choice Assay

To explore how *Lema* beetles respond to *M. sexta*-infested plants, we performed a two-choice assay in a cage (62 × 39 × 39 cm^3) at 25 °C, 70% relative humidity. Five newly-molted third instar caterpillars were placed on a plant and were allowed to feed for 3 days. The control plants were healthy plants of similar size. Treated and control plants were placed 20 cm apart from each other inside the cage. A pair of *Lema* beetles were introduced into the cage and were allowed to feed and oviposit for the following 72 h. The number of eggs on each plant and the plant the adult *Lema* beetles consumed more of were recorded after the experiment. Those pairs of *Lema* beetles that did not lay any eggs were excluded from the data analysis.

Performance of *M. sexta* Larvae

To monitor *M. sexta* larvae performance, a single neonate was transferred to a petri dish that was supplied with either healthy or beetle-infested *Datura* leaf discs (diameter = 2 cm), and an artificial food disc as control. Twenty caterpillars were used for each treatment. We sprayed distilled water on filter paper and refreshed the leaf discs as well as the artificial food every day. Both leaf discs and artificial food were sufficient during the experiment. The length and mass of larvae were measured after 7 days. In the meantime, we assessed the larvae performance on intact beetle-infested and control *Datura* plants. We placed five neonates on each caged plant and watered the plants every day with 200 ml water, respectively. Twenty caterpillars and four plants were used for each treatment. After 7 days, the length and mass of the larvae were measured. All the caterpillars were alive during the assay in both paradigms. In addition we raised caterpillars on discs of artificial food, healthy control plants, or beetle infested plants until pupation and measured pupal weight afterwards.

Volatile Chemical Analysis

We collected volatiles from four groups of *Datura* plants: healthy, mechanically damaged, *M. sexta*-infested, and beetle-infested. Ten adult beetles and five newly molted third instar *M. sexta* caterpillars were allowed to feed on *Datura* plants for 3 days and together with their feces were later removed before odor collection. Mechanical damage was created by using a pattern wheel right before odor collection. Thirty grams of leaves from those four groups were put into a 500 ml glass bottle. Ambient air flowed (300 ml min^{-1}) into the bottom of the bottle primarily through a charcoal trap and was pulled out (200 ml min^{-1}) through a glass tube (ARS) containing glass wool and 20 mg of Super Q (Alltech). Airflow was created by a manifold vacuum pump (model DAA-V114-GB; Gast Manufacturing). Volatile emissions from the enclosed leaves were trapped for 24 h. Immediately after collection, traps were eluted by spiking each with 10 μl of diluted 1-bromodecane (1:10^5 in hexane) as an internal standard and flushing the trap with 600 μl of Hexane into a GC vial containing a glass insert. The samples were analyzed by GC-MS (Agilent 6890 GC & 5975C MS, Agilent, USA) equipped with a 30-m DB-Wax column (ID 0.25 mm, df 0.25 μm; Supelco). One microliter was injected into a 250 °C injector. The column temperature was maintained at 40°C for 1 min and then increased to 260°C at 20°C min^{-1}, followed by a final stage of 10 min at 260°C. Compounds were identified by comparing mass spectra against synthetic standards and NIST 2.0 library matches. The numbers in the GC-MS chromatograms refer to the following compounds: (1) 3-hexanone; (2) 2-hexanone; (3) 3-hexenal; (4) 2-heptanone; (5) 3-hexanol; (6) (*E*)-2-hexenal; (7) β-ocimene; (8) methyl heptanoate; (9) tridecane; (10) *cis*-3-hexenyl acetate; (11) 1-hexanol; (12) *cis*-3-hexen-1-ol; (13) *cis*-2-hexen-1-ol; (14) tetradecane; (15) 1-octen-3-ol; (16) *trans*-3-hexenyl butyrate; (17) 2-ethyl-1-hexanol; (18) α-copaene; (19) Internal standard (1-bromodecane); (20) *trans*-α-bergamotene; (21) β-caryophyllene; (22) *cis*-3-hexenyl hexanoate; (23) *cis*-3-hexenyl lactate; (24) α-acorenol; (25) α-farnesene; (26) squalene; (27) benzyl alcohol. All of the synthetic odorants that were tested and confirmed.

Non-volatile Chemical Analysis

Datura plants were infested with either ten beetles or five newly molted third instar *M. sexta*. After 3 days, 5 - 6 leaves of each plant were collected (one leaf per sample) in 50 ml Falcon tubes and were immediately frozen with liquid nitrogen. Untreated *Datura* plants were used as control. Both treated and control plant material was lyophilized over 5 days and subsequently ground to a fine powder using 3 mm diameter steel beads (20 g per sample) in a paint shaker (3 min).

For amino acid quantification, around 10 mg tissue from each sample was extracted with 1 ml 80% (v v^{-1}) MeOH and agitated on a horizontal shaker for 10 min. After centrifugation at 18000 g for 10 min, 800 μl supernatant was transferred into a new centrifuge tube. Afterward, 50 μl raw extract was mixed with 450 μl water containing 10 μg ml^{-1} [^{13}C, ^{15}N] labeled algal amino acids (Isotec, Miamisburg, USA) as internal standards.

For targeted and non-targeted chemical analysis of *Datura* tropane alkaloids, 1 ml 80% (v v^{-1}) MeOH either with or without 4 μg ml^{-1} caffeine (AlfaAesar, Kandel, Germany) as internal standard were used for 10 mg dried leaf powder extraction, respectively. Samples then were vortexed (5 sec), sonicated (10 min), vortexed again (5 sec), and centrifuged (5 min, 15000 rpm, 4°C). Subsequently, 100 μL of the supernatant was transferred into another vial, and 900 μL of 80% MeOH was added. Ultimately, samples were subjected to chemical analysis.

The measurement of amino acids was performed on a QTRAP 6500+ triple quadrupole mass spectrometer (AB Sciex LLC, Framingham, MA, USA) coupled to the LC system using the multiple reaction monitoring (MRM) parameters and separation gradients described previously.[38] The concentration of individual amino acids was determined by comparison with respective

U-13C, -15N-labeled amino acid internal standard except for tryptophan and asparagine. Tryptophan and asparagine were quantified using labeled phenylalanine and aspartate using the experimentally determined response factor 0.42 and 1.0, respectively.

Non-targeted, ultra-high-performance liquid chromatography-electrospray ionization–high-resolution mass spectrometry (UHPLC–ESI–HRMS) was performed with a Dionex Ultimate 3000 series UHPLC (Thermo Fisher Scientific, Waltham, MA, USA) and a Bruker timsToF mass spectrometer (Bruker Daltonik, Bremen, Germany). UHPLC was used applying a reversed-phase Zorbax Eclipse XDB-C18 column (100 mm × 2.1 mm, 1.8 μm, Agilent Technologies, Waldbronn, Germany) with a solvent system of 0.1% formic acid (A) and acetonitrile (B) at a flow rate of 0.3 ml min^{-1} and an oven temperature of 25°C. The following gradient was applied to achieve separation: 0 to 0.5 min, 5% B; 0.5 to 11.0 min, 5% to 60% B in A; 11.0 to 11.1 min, 60% to100% B, 11.1 to 12.0 min, 100% B and 12.1 to 15.0 min 5% B. Ionization was achieved using electrospray ionization (ESI) in positive ionization with the following parameters: capillary voltage 4.5 KV, end plate offset of 500 V, nebulizer pressure 2.8 bar, nitrogen at 280°C at a flow rate of 8 L min^{-1} as drying gas. Mass spectra were recorded for a mass range from m/z 50 to 1500. At the beginning of each chromatographic analysis, 10 μl of a sodium formate-isopropanol solution (10 mM solution of 50% NaOH in isopropanol (v v^{-1}) water containing 0.2% formic acid) was injected into the dead volume of the sample injection for re-calibration of the mass spectrometer using the expected cluster ion m/z values.

Quantification of atropine ((±)-hyoscyamine) and (-)-scopolamine (standards were purchased from AlfaAesar, Kandel, Germany, and Sigma-Aldich Chemie GmbH, Taufenkirchen, Germany, respectively) was achieved on an Agilent 1260 Infinity II LC system consisting of a binary pump G7112B, an autosampler G7167A, and a column thermostat G7116A (Agilent Technologies). Chromatographic separation was carried out on a ZORBAX Eclipse XDB-C18 column (50 x 4.6 mm, 1.8 μm) from Agilent Technologies. A binary solvent system was used as a mobile phase consisting of A) 0.05% formic acid and B) acetonitrile with a constant flow rate of 1.1 ml x min^{-1} at 20°C column temperature. The following gradient was applied: 0-0.5 min, 10% B; 0.5-4.0 min, 10-90% B; 4.0-4.02 min, 90-100% B; 4.02-4.5 min, 100% B; 4.5-4.51 min, 100-10% B; 4.51-7.0 min, 10% B. The column outlet was connected to a QTRAP 6500+. The Turbo Spray IonDrive ion source was running in positive ionization mode with 4500 V ion spray voltage and 650 °C turbo gas temperature. The curtain gas was set to 40 psi; the collision gas to 'low' and both ion source gases 1 & 2 were set to 70 psi. Scheduled multiple reaction monitoring (scheduled MRM) was used to monitor analyte parent ion → product ion fragmentations as follows: *m/z* 304 → 138 (retention time (R_t) 1.95 min; collision energy (CE) 25 V) for (-)-scopolamine; *m/z* 195 → 138 (R_t 2.19 min; CE 27 V) for caffeine; *m/z* 290 → 124 (R_t 2.51 min; CE 33 V) for atropine. Both Q1 and Q3 quadrupoles were maintained at unit resolution. Analyst 1.6 software (Applied Biosystems) was used for data acquisition and processing. Caffeine was used as an internal standard for quantification. The response factors related to the analyte alkaloids have been experimentally determined as follows: response factor (*f*) 7.60 for atropine *and* (*f*) 4.91 for (-)-scopolamine.

Caterpillar Fitness With Enhanced Amino Acid Concentrations

To test whether the high concentrations of threonine explain the disadvantage of caterpillar performances, we experimentally enhanced the concentration of selected amino acids in *Datura* leaves, 10 μl of an amino acid-ddH_2O solution was pipetted onto 16 mm leaf discs before the discs were offered to the caterpillars, a revised protocol from Lackner et al.[39] The concentrations of threonine and glutamine applied to the leaf surfaces were based on the mean concentrations in beetle-infested *Datura* leaves measured after 3 days. Control leaf discs were treated with ddH_2O only. Amino acid-coated leaf discs and control leaf discs were placed in Petri dish arenas and refreshed every day as abovementioned. The length and mass of larvae were measured after 7 days.

Parasitoid Wasp Y-maze Assays

To test the effect of volatiles emitted by *Lema* beetle-infested *Datura* plants on *C. congregata* behavior, we conducted a Y-tube olfactometer assay in the absence of any visual cues. The Y-tube olfactometer (stem, 9 cm; arms, 10 cm at 60° angle; internal diameter (ID), 2.3 cm). Purified and humidified air entered each odor source bottle (500 ml) at 0.5 liter/min (adjusted by flow meters; Analytical Research System) via Teflon tubing and carried the volatile organic compounds through the connector tube to the arms of the olfactometer. The air was evacuated at the stem end at 1 liter min^{-1} (adjusted by flow meters; Analytical Research System). 15 grams of leaf tissues were collected from control, *M. sexta*-infested (infested by 5 newly-molted third instar caterpillars for 3 days) and *M. sexta*-beetle-infested (infested by 5 newly-molted third instar caterpillars and 10 beetles for 3 days) plants. The system was left connected for half an hour before releasing wasps at the entrance of the Y-tube olfactometer. Experiments were conducted according to Wei and Kang[40] with some modifications. Each three-day-old mated female parasitoid was introduced into the Y-tube at the entrance of the stem and thus had a choice between the treatment and the control. A parasitoid was considered to have made the first choice when it moved >3 cm into either arm (visually assessed by a line marked on both arms). Parasitoids' final choice was the arm they were in at the end of the 5-min experimental period. The amount of time parasitoids spent in each arm of the device was also recorded. We reversed the position of treatment and control after every five individuals and replaced the Y-tube after 10 tests. We excluded the wasps that did not make any choice within 5 min from data analysis.

Parasitoid Wasp Tent Assays

To test the parasitism rate of *C. congregata*, we conducted a tent (47.5 × 47.5 × 47.5 cm) assay. On one side, a second-instar caterpillar was placed in a petri dish with a leaf that was already infested by caterpillars. On the other side, another second-instar caterpillar was placed in a petri dish with a leaf that was already infested by beetles and caterpillars (beetles were present during the experiment). Two Petri dishes were 30 cm apart. The experiments were conducted for 15 min. Caterpillars were kept separately after all the tests. The number of cocoons emerged from individual caterpillars was recorded.

Generation of Antisense Riboprobes for In Situ Hybridization

To generate an antisense riboprobe for Orco and Or35, PCR fragments were amplified from antennal cDNA. The resulting PCR fragments were cloned into TOPO TA Cloning Vector (ThermoFisher, Waltham, Massachusetts, USA) and was subjected to sequence analysis. The digoxigenin-labeled antisense riboprobe for Orco and Or35 were generated from this plasmid insertion by using the T7/SP6 RNA transcription system (Roche Diagnostics, Mannheim, Germany) as recommended by the manufacturer.

In Situ Hybridization

With few modifications, in situ hybridization experiments were performed using the protocol described in detail previously.[41] For tissue preparation, antennae of female *M. sexta* were surgically removed and embedded in Tissue-Tek O.C.T. Compound (Sakura Finetek, Alphen aan den Rijn, The Netherlands). Longitudinal sections (12 μm thick) through the antennae were prepared with a Cryostar NX50 cryostat (Thermo Fisher Scientific, Waltham, Massachusetts, USA) at − 20 °C. Sections were thaw-mounted on Super Frost Plus slides (Menzel, Braunschweig, Germany) and immediately used for in situ hybridization experiments. Briefly, sections were immediately transferred into a fixation solution (4% paraformaldehyde in 0.1 M $NaHCO_3$, pH 9.5) for 22 min at 4 °C. Next, sections were washed in 1xPBS (0.85% NaCl, 1.4 mM KH_2PO_4, 8 mM Na_2HPO_4, pH 7.1) for 5 min, incubated in 0.2 M HCl for 10 min and washed twice in 1xPBS for 2 min each. Then sections were incubated for 10 min in acetylation solution (0.25% acetic anhydride freshly added in 0.1 M triethanolamine) followed by 3 wash steps in 1xPBS (each wash step lasted for 5 min). Sections were incubated in pre-hybridization solution [5xSSC (0.75 M NaCl, 0.075 M sodium citrate, pH 7.0) and 50% formamid] for 10 min. For hybridization, each slide was subsequently covered with 130 μl hybridization solution 1 [50% formamide, 25% H_2O, 25% Microarray Hybridization Solution Version 2.0 (GE Healthcare, Freiburg, Germany)] containing the labeled antisense RNA probe. After placing a coverslip, slides were incubated in a humid box (50% formamide) at 60 °C overnight. Visualization of digoxigenin-labeled Or35 in non-fluorescent in situ hybridization experiments was performed using an anti-digoxigenin alkaline phosphatase-conjugated antibody (Roche Diagnostics) diluted 1:500 and a substrate solution containing NBT (nitroblue tetrazolium) and BCIP (5-brom-4-chlor-3-indolyl phosphate). Tissue sections were analyzed with a Leica DMLB microscope (Leica, Microsystems, Wetzlar, Germany) equipped with a Canon EOS 700D camera (Canon, Tokyo, Japan).

Fluorescence in situ hybridization (FISH) experiments using digoxigenin-labeled antisense riboprobes were conducted as described recently.[42] A fluorescent anti-HRP antibody, recognizing neuron-specific glycoproteins in insects,[43] was applied for better visualization of antennal neurons (green). Before mounting, counterstaining was performed with goat-anti-HRP Alexa Fluor 647-conjugated antibody (1:200) (Jackson ImmunoResearch, Ely, Great Britain) in 1x TBS (0.1 M Tris, 0.15 M NaCl, pH 7.5)] for 30 min at room temperature followed by washing with distilled water for 5 min. Sections were analyzed with a confocal LSM 880 laser scanning microscope (Carl Zeiss). Confocal image Z-stacks were acquired from antennae in the red and green fluorescence channels along with the transmitted light channel. In these figures, the red and green fluorescence channels that are overlayed with the transmitted light channel are shown separately or as merged images.

Single Sensillum Recording (SSR)

Odorants for SSR analysis were selected based on compounds structurally similar to α-copaene. 10 μl of diluted odor ($1:10^2$) or solvent alone (DMSO) were pipetted onto a circular filter paper (diameter: 12 mm) and placed into a glass pipette. In addition, we performed SSR according to the methods described before.[44] Unlike the antenna of the fruit fly, which contains ∼ 450 olfactory sensilla,[45] the antenna of female *M. sexta* has about 10^5 sensilla.[46] This makes recording from all sensilla impossible. Based on previous literature,[14,44] we decided to randomly test basiconic and trichoid sensilla from the 14th and 15th distal segments of female antennae while stimulating the contacted OSNs with α-copaene. Sensilla were identified by their characteristic morphology.[46] When the tested sensilla elicit a response to α-copaene, we continued to test the sensilla with seven other terpenes, otherwise, we changed to another sensillum. In total, 140 basiconic sensilla and 20 trichoid sensilla were tested. Responses were quantified by counting all spikes recorded from individual neurons.[47,48] The response was calculated as the difference in spike number observed 1 s before and after the stimulus onset. Both the baseline activity and the response to solvent (DMSO) were subtracted.

Odorant Exposure, Tissue Collection, and RNA Extraction

To predict the candidate odorant receptors that might be involved in α-copaene detection, we took the approach of DREAM (Deorphanization of receptors based on expression alterations in mRNA levels) technique. Two hours after onset of scotophase, a three-day-old virgin female *M. sexta* was exposed to α-copaene for 6 hours in a 500 ml glass bottle with a concentration of 10^{-2} (v v^{-1}) dissolved in DMSO (Dimethyl sulfoxide). A virgin female *M. sexta* exposed to DMSO was the Control. To avoid physical contact of *M. sexta* with the chemicals, 20 μl of the odorant or solvent, respectively, were applied into a PCR well (200 μl) with holes on the lid. The antenna was cut off and placed into liquid N_2 immediately after the exposure ended. Total RNA for each replicate and treatment was extracted using an unbiased RNA isolation kit (Direct-zol RNA MiniPrep, Zymo Research). RNA quality was measured with a *NanoDrop* spectrophotometer (Thermo Fisher Scientific). Total RNA was stored at −80 °C until further use.

Nanostring Assay

NanoString nCounter assays were performed according to the manufacturer's standard protocol and raw data were normalized using nSolver Analysis Software version 4.0 (NanoString Technologies, Seattle, WA, USA) for further analysis. The reaction was carried out with 100 ng of the total RNA isolated as described above. We used RPL31 (Ribosomal Protein L31) and RPL19 as the

housekeeping genes. The raw output.RCC files are available upon request. Pre-processing was performed as instructed by Nanostring for background correction. Samples with normalization flags were removed before the final analysis.

Gene Cloning

The five candidate *Or* genes (*Or19*, *Or26*, *Or31, Or35*, and *Or67*) and *Orco* along with two randomly selected *Ors* (*Or9* and *Or10*) were cloned with specific primers (STAR Methods) designed by Primer5.0 (PREMIER Biosoft International, CA, USA). The PCR was performed in 25 μl containing 12.5 μl of 2 × Phanta Max Master Mix (super fidelity), 9.5 μl of ddH_2O, 1 μl of cDNA template, and 1 μl forward and reverse primers (10 μM). The PCR conditions were 95 °C for 3 min; 35 cycles of 95 °C for 15 s, 55 °C for 15 s, 72 °C for 90 s; 72 °C for 8 min. PCR products were run on a 1.2% agarose gel, and the band was recovered and purified by AxyPrep DNA Gel Extraction Kit (Axygen, Suzhou, China). Purified PCR products were cloned in the pEASY-Blunt3 Cloning Vector (TransGen Biotech, Beijing, China) and then transformed into Trans1-T1 Phage Resistant Chemically Competent Cells (TransGen Biotech, Beijing, China). The transformants were screened on LB-Agar plates containing 100 μg ml^{-1} ampicillin. The positive clones were sequenced by the company Tongyong (Chuzhou, China). *Or31* had a premature stop codon caused by partial sequence deletion comparing to the annotated sequence, therefore it was excluded for further test.

Vector Construction and cRNA Synthesis

The ORFs of six *Or* genes and *Orco* gene were amplified using primers with a cutting site of EcoRI or XbaI (STAR Methods) and were then cloned into pGH19 vector that was double-digested with EcoRI and XbaI, using the ClonExpress Ultra One Step Cloning Kit (Vazyme, Nanjing, China). The plasmid was extracted by the Miniprep method and purified with phenol-chloroform-isoamyl alcohol. The purified plasmid was linearized with a restriction enzyme (NotI/NdeI) and used as template to synthesize cRNAs by using T7 polymerase of mMESSAGE mMACHINE T7 Kit (Thermo Fisher Scientific, Waltham, MA, USA). The purified cRNAs were diluted with nuclease-free water at a concentration of 2 μg μl^{-1} and stored at −80 °C until use.

Receptor Expression in *Xenopus* Oocytes and Two Electrode Voltage Clamp Electrophysiological Recordings

The six Ors were expressed in *Xenopus* oocytes and ligand sensitivity was detected using two-electrode voltage clamps as previously reported.[49] The 1 M stock solutions in dimethyl sulfoxide (DMSO) were prepared and stored at −20 °C. The stock solution was diluted in Ca^{2+} free standard oocyte saline (SOS) buffer (100 mM NaCl, 2 mM KCl, 1.8 mM $CaCl_2$, 1 mM $MgCl_2$, 5 mM HEPES, pH 7.6) before the experiments. All chemicals were freshly prepared at the concentration of 10^{-4} M for the experiments. For each chemical, 10 oocytes (replicates) were tested in the screening tests. Oocytes injected with sterilized ultrapure H_2O were used as controls.

QUANTIFICATION AND STATISTICAL ANALYSIS

Differences in total volatiles emissions were analyzed using non-parametric Kruskal–Wallis analysis of variance followed by Mann–Whitney tests (Raw p values, uncorrected significance) for multiple pairwise comparisons. The chemical profiles of different *Datura* hosts headspaces were compared by one-way ANOSIM using Bray–Curtis dissimilarity matrix (PAST Version 3.25). Data processing of tropane alkaloid chemical analysis was achieved with RStudio (Version 1.3.1093). Generalized least squares models with varIdent variance correction were used to test for significant differences in atropine and (-)-scopolamine levels between the treatments. Factor level reduction was applied as post-hoc test, using a confidence level of 95%. All other statistical analysis and plotting were made in RStudio (version 1.3.1093; R version 3.5.1). Normality test was assessed on datasets using a Shapiro test. If datasets for a given experiment were normally distributed, t-test/anova was performed; otherwise, Wilcoxon rank-sum test/ Kruskal-Wallis test was performed.

Bucketing of the non-targeted analysis data was carried out using MetaboScape (Bruker Daltonik, Bremen, Germany) applying the T-Rex 3D algorithm for LC-qTOF data. Peaks were defined with an intensity threshold of 3000 and a minimum length of 10 spectra within a time window from 0.4 to 11 min. Feature extraction was applied on peaks with a minimal peak length of 8 spectra and an abundance in at least 6 of the 18 samples. Adducts of $[M+H]^+$, $[M+Na]^+$, $[M+K]^+$, $[M+NH_4]^+$ and $2[M+H]^+$ were grouped as a single bucket if they had an EIC correlation of 0.8. Features correlating to reference spectra of atropine and (-)-scopolamine were tagged in the resulting peak table, correspondingly.

The peak table was exported as.csv-file and further processed, using the MetaboAnalyst 5.0 online platform (https://www.metaboanalyst.ca). After an interquantile filtering and data normalization, based on sample weight and a pareto scaling, chemometric analysis (one-way ANOVA, PCR and PLS-DA) of the peak table was performed using the corresponding functions in the online tool. Figures were then processed with Adobe Illustrator CS5.